Contributed Papers in Commemoration of the Establishment
of the Young Researcher Encouragement Award

Uncovering the Nature of Chaos

YoshisukeUeda

The Japan Society for Industrial and Applied Mathematics
Applied Chaos Research Group

For young researchers who are interested in the field of nonlinear science and technology

I was directly guided by Dr. Hiroshi Shibayama in the master's course, and because of his personality and the fun and enjoyment of the research he taught me, I entered a doctoral course, which I had not expected before, and started my career as an educator and researcher. The outline of what has happened since then is described in "Strange Attractors and the Origin of Chaos" (see URL in footnote 1 of the main text).

As mentioned in the report, in the late 1970s, I had the opportunity to expand the scope of my research on nonlinear phenomena to include various phenomena in the field of electric power, and during the period when the whole world was focused on chaos research, I was engaged in research in the field of electric power engineering.

In the early stages of my development as a researcher, I was involved in low-speed analog computer experiments, and as an educator and researcher, I was able to engage in experimental research on synchronous generators and simulated power systems when I had gained some understanding of the actual conditions in this field.

Although many people consider the author a theorist, he himself is a believer of "the truth resides in actual phenomena" and he knows that without actual data to support anything he does, he will not be able to feel the satisfaction of having understood it. However, during the series of work on this contributed paper, I realized the horror of "being satisfied with a superficial understanding" when what I had understood so far was shaken. Therefore, I would like to ask you to consider this contributed paper strictly as a work in progress.

I would like to express my best wishes for the continued development of young researchers.

Yoshisuke Ueda

ISSUE DATE: 27 November 2023

URL:
https://chaos.amp.i.kyoto-u.ac.jp/en/wp-content/uploads/2023/11/UNCyu.pdf

Uncovering the Nature of Chaos

Yoshisuke Ueda*

1. Outline of this Paper

In the spring of 2022, the author published a monograph of his major entitled "Theory of Chaotically Transitional Phenomena (in Japanese)," from Japan Printing Publishing Co., Ltd (URL; https://jpp.co.jp/).

The text is an abridged translation of the above book. Since our goal was to keep the text compact, we cannot deny that some of the explanations are a bit rough. However, we believe that the reader who understands this abridged translation will have a rough understanding of the figures and numerical values in the original document. We are planning to publish the original book in English, with additional revisions and additions.

Chaotically transitionnal phenomena are real steady states with irregularities (stochastic processes) in deterministic systems, which were proposed prior to chaos phenomena (1973). However, since this concept conflicts with the "separation (or, deviation) concept", it was completely ignored before the rise of the field, starting with May's (1974), and, Li and Yorke's CHAOS (1975).

To tell the truth, the author did not know the concept of separation (or deviation) at that time. It seems that it was a well-known concept in philosophy, and if the author had known it, he probably would not have dared to go against the well-known common sense, which greatly contradicted his understanding, and he might have avoided the proposal of the term "chaotically transitional oscillations" in his paper [1] *1. However, his confidence in the experimental results did not waver from his theory.

* Emeritus Professor, Kyoto University, Japan

*1 The numbers in parentheses indicate the numbers of the references, but in this abridg-

On November 27, 1961, the author encountered chaotically transitional oscillations while engaged in an analog computer experiment [*2]. In the nonlinear oscillation theory at that time, the stationary state, dynamic periodic oscillation, and quasi-periodic oscillation were well known as the steady state in various non-linear oscillatory systems. These phenomena are described by equilibrium points, limit cycles of autonomous systems, fixed points, periodic points, and invariant closed curves of non-autonomous periodic systems (i.e., maps or transformations defined by solutions of the equations). Moreover, these are all deterministic phenomena. However, chaotically transitional oscillations are neither steady-states nor ordered (deterministic) phenomena above-mentioned.

The steady-state point sequences (or, stroboscopic observation sequences) that chaotically transitional oscillations produce on the 2-dimensional phase plane are not regular in the sense that they produce a simple closed curve. It was well known that the quasi-periodic oscillations produced a simple closed curve and that there was a regularity in the order of the representative points that appeared on it (see differential equations on the torus and rotation number).

In other words, even if the chaotic point sequences were (forcibly) rearranged to appear on a simple closed curve (even if approximated), the order of the representative points appearing on the curve would exhibit a behavior different from that of the rotation number of a quasi-periodic oscillation.

The "fundamentally different property" that always appears in analog computer experiments keeps on telling us that "chaotically transitional oscillations are not quasi-periodic oscillations" [*3].

---

ment, the references are numbered the same as in the original, so the list of references has been omitted. The main references, e.g., [1] and [44], are in Japanese, but their English translations [1] Ueda_03.pdf, and, [44] Ueda_02.pdf, can be found in the following URL;

https://repository.kulib.kyoto-u.ac.jp/dspace/handle/2433/71101

[*2] The results of the analog computer experiment (original data set) are archived at the Brookheaven National Laboratory, New York.

The data number of the Broken Egg Attractor observed by chance on November 27, 1961 is BNL Photography Division Negative No. 1 - 380 - 90.

The author's recollection (in Japanese) of the analog experiment is as follows:

"Identity of Mystery Appeared in between Entrainment and Quenching Phenomena — Parameter Value in the NLP Report Says It All —" in Fundamental Reviev, IEICEJ, Vol. 7, No. 3, pp. 172-185 (2014)

[*3] In fact, at that time, the author thought that this phenomenon appears only in forced

The educational program in which the author grew up is in the field of electrical and electronic engineering. It is a technical field that focuses on the application of known phenomena rather than on the theoretical construction of principles and principles of natural phenomena themselves. Perhaps a combination of the environment in which the author was raised and his own proclivities, he was unconsciously instilled with an awareness of the need to first identify the mechanisms and properties of phenomena, rather than focusing on the distinction between ordered (deterministic) and irregular phenomena from a bird's eye view and theoretically.

From the theory of nonlinear oscillations, we have learned that a point set on the phase plane representing stationary and dynamic real steady states phenomena mentioned above must have structural stability in addition to asymptotic stability. However, not only the structure of the point set representing the mysterious chaotic oscillations but also the stability conditions imposed on the set (fluctuations of the system strictly existing in the real system, i.e., the structural stability) became the object of his interest, and at the same time, he was struck by the horror of the problem.

The experimental results up to this point and the record of these discussions are given in Refs [1, 44]. The authors attempted to explain the experimental results in applied mathematical terms, but neglected to describe the structural stability of the chaotic oscillations. The discussion in these literatures is based on the assumption that the systems studied in these literatures are structurally stable. This was a concern of the author at the time of writing, but was easily compromised based on the fact that various numerical results were in good agreement with the analog computer experiments. In the literature, the term "attractor" is not used in the descriptions (in Japanese), and the descriptions are often repetitive and roundabout. This is a proof that the author did not know the term "attractor" at the time of writing. It is puzzling in retrospect, but the past literature cannot be helped.

Here, let us recall the situation of computers in the 1960s. It was 1962 when

---

self-oscillatory systems, although it was different from quasi-periodic oscillation. Soon, however, the author became convinced that troublesome and disturbing oscillations also appear in forced oscillatory systems that did not exhibit self-excited oscillations (the background is described in [46] Ueda_07.pdf).

the author first used a digital computer (Kyoto University Digital Computer KDC-I). Writing programs in machine language was an extremely tedious job. The RKG method was mainly used to solve the second-order Duffing equation (a nonautonomous periodic 2D-system with period 2π) as described below. For the solution with $\Delta t = 2\pi/120$ increments of independent variable, it took almost one minute (about 60 seconds) to calculate the solution curve for one period 2π.

Under such a research environment, analog computers have played a leading role in the simulation of nonlinear ordinary differential equations. The numerical experiments presented in this article were conducted using general-purpose desktop digital computers in the 2010s. At the time of writing Refs [1, 44], it was an unrealized dream to perform the numerical experiments shown in this article.

Around a little more than a century before the existence of computers, Poincaré and Birkhoff and his colleagues seemed to have drawn in their minds the equivalent of the numerical results of the experiments described in this document, either by intuition or by thought [*4]. Shortly thereafter, Andronov and Pontryagin proposed a necessary and sufficient condition for structural stability.

We cannot help but admire and admire their achievement, which was made in the age when there were no computers.

In the following sections, the Duffing equation is taken as a two-dimensional nonautonomous periodic system, and the results of numerical experiments for representative coefficient values, as well as some hypotheses and predictions based on the experimental results, are presented.

2. Summary of Experimental Results and Discussion

This Chapter is a summary of Chapters 3 and 4 of the original. As mentioned earlier, it is boldly simplified to describe the main points from a bird's-eye view of the original book.

[*4] The concepts underlying the theory of this paper owe much to Birkhoff and Smith, "Structure Analysis of Surface Transformations" (1928). In the descriptions in this article, we have used the old terminology (used by Birkhoff and others) rather than the scientific terminology used in recent dynamical systems theory.

Therefore, the flow of the topics was subject to a certain degree of continuity. In other words, the subject matter (or the point of contention) changed when the paragraphs were changed. Although a section should have been added, there was no such discontinuity, which is not in line with the intended purpose of this document. This dilemma can be resolved by simply making the readers aware of this situation.

2.1 Objects of numerical analysis, equations and chaotic phenomena

The following Duffing equations, which are typical in the theory of nonlinear oscillations, are used in the experiments.

$$\left.\begin{array}{l} \dfrac{dx}{dt} = y, \quad \dfrac{dy}{dt} + k\,y + x^3 = B\cos t \\ \text{where } k\text{: damping coefficient}, B\text{: forced amplitude} \end{array}\right\} \tag{1}$$

Chaotically transitional oscillations (phenomena) are observed in the real system represented by this deterministic equation. Among chaotic oscillations, UCA (Ueda's Chaotic Attractor) is the attractor when the constant value of the system is set to $k = 0.05$, $B = 7.5$ [*5].

The expression "UCA system" appears frequently in the text and refers not only to equation (1) with the constant (k, B) value of (0.05, 7.5) but also to the case where the value of (k, B) is close to (0.05, 7.5); the same applies to the UCA. When limited to the former case, we sometimes refer to it as "representative UCA system". Also, the UCA system is an equation of class D in the sense of Levinson.

Fig. 1 Chaotic attractor UCA

Figure 1 represents a representative UCA. The figure depicts the (computer) solution of the representative UCA system, i.e., 100,000 representative points representing the steady state of the discrete dynamical system defined by the solutions of the UCA system (precisely the computer representative point at $t = 2n\pi$ (n : integer), or the image of a discrete dynamical system by successive iterative mappings).

[*5] For explanations of the terminology and questions (with simplified descriptions), please refer to the original document and the references cited therein.

What this Figure 1 suggests (or infers from it) is that the real disk represents a single stroboscopic observation point, but there exists a theoretical disk (circle neighborhood) centered on the representative point on the UCA in the neighborhood of the real disk, where an infinite number of central points exist.

The central point is a saddle-type periodic point, or an accumulation point of recurrent points in a chaotic attractor. In general, the minimal set (consisting of recurrent points) is the smallest unit that represents the steady-state solution [*6].

2.2 Steady state represented by the representative UCA system

Figure 2 shows the maximum finite invariant set Δ and the surrounding curve Γ_n for a representative UCA system. In general, the maximum finite invariant set contains all the steady states, i.e., attractors, represented by the system. The figure shows that there exists only one attractor in the system and that the sequence of closed sets Δ_n enclosed by the surrounding curve Γ_n is an iterated sequence of contraction mappimg, which converge to the maximum finite invariant set Δ at $n \to +\infty$.

Fig. 2 Maximum finite invariant set of UCA system

The number of surrounding curves in Fig. 2 is small and not sufficient to clarify the state of convergence, but it is impossible to draw a sufficient figure. Therefore, we would like you to infer from the figure how the beards and folds of the surrounding curve Γ_n penetrate into the gaps of the UCA as far as possible.

The figure shows that UCA is a maximum finite invariant set Δ. Also, the fact that the damping coefficient value of the system (1) is positive ($k > 0$) implies that "the area of UCA is zero".

In the following sections, we present the results of the numerical analysis performed to elucidate the structure of the UCA.

2.3 Structure of the representative UCA

[*6] If there is no recurrent point that differs from the periodic point, the recurrent point is the periodic point.

Regardless of the presence or absence of a recurrent point that is different from the periodic point, the content described in this paper remains the same.

There exist uncountably many saddle-type periodic points in UCA, each of which has α and ω branches. If the period of the periodic point of interest is n, its α branch and ω branch are invariant sets with respect to n iterated maps (n-periodic branches).

2.3.1 Fixed points of the representative UCA and their invariant branches

The UCA has three saddle-type fixed points. Their coordinates and characteristic numbers ρ_1, ρ_2 are as follows.

$$\left.\begin{array}{ll} \mathrm{D}\,(2.891363,\ 0.246965) & 13.003744,\ 0.056169 \\ {}^{1}\mathrm{I}\,(3.170688,\ 0.295115) & \text{-0.490535, -1.488991} \\ {}^{2}\mathrm{I}\,(2.273854,\ \text{-0.260323}) & \text{-0.490535, -1.488991} \end{array}\right\} \quad (2)$$

The upper panel of Figure 3 shows the root of the invariant branches (α and ω branches) of the directly unstable fixed point D. The lower panel shows a somewhat extended version of the invariant branches in the upper panel superimposed on the computer UCA (black circle is directly unstable fixed point D, white squares are inversely unstable fixed points ${}^{1}\mathrm{I}$ and ${}^{2}\mathrm{I}$).

Fig. 3 Invariant branches of the saddle fixed point D on UCA

As Figure 3 shows, the α_1 (or, α_2) branch intersects the ω_1 and ω_2 branches. In the same way, the ω_1(or, ω_2) branch intersects the α_1 and α_2 branches.

2.3.2 Invariant branches and homoclinic structures of the fixed point D

As mentioned above, the dilectly unstable point D has four possible homoclinic structures A(α_1, ω_1), B(α_1, ω_2), C(α_2, ω_1) and D(α_2, ω_2). Here we first present the results of our experiments on the homoclinic structure of invariant branches for type A and type B.

Fig. 4(a) α_1, ω_1 homoclinic structure (Type A)

and,

Fig. 4(b) α_1, ω_2 homoclinic structure (Type B)

Figure 4(a), or 4(b), is not two figures, but an illustration of the symbols and curve thicknesses that should be inserted in the lower figure (the upper figure is drawn so that it overlaps the lower figure if it is moved directly down).

In these figures, the invariant branch depicted by the bold line in the upper

panel is called the basic homoclinic cycle (point D is the directly unstable fixed point and the homoclinic point 0_b is the cusp point).

The homoclinic points $0_a, 0_b, 1_a$ in Fig. 4(a) and the points $0_a, 0_b, 0_c, 0_d, 1_a$ in Fig. 4(b) are called the basic homoclinic points (point 1_a is the image of point 0_a) [*7].

Let $0_a, 0_b, 1_a$, in Fig. 4(a) be ${}^{\mathrm{A}}0_a, {}^{\mathrm{A}}0_b, {}^{\mathrm{A}}1_a$, and $0_a, 0_b$, $0_c, 0_d, 1_a$, in Fig. 4(b) be ${}^{\mathrm{B}}0_a, {}^{\mathrm{B}}0_b, {}^{\mathrm{B}}0_c, {}^{\mathrm{B}}0_d, {}^{\mathrm{B}}1_a$, and we should distinguish between type A and type B. However, in the case where the different types of homoclinic points are not depicted on a single leaf, we have used a concise expression.

The subsequent figures 4(c) and 4(d) show the experimental results for type C and D, respectively, and are plotted according to the above.

Fig. 4(c) α_2, ω_1 homoclinic structure (Type C)

and,

Fig. 4(d) α_2, ω_2 homoclinic structure (Type D)

Note that although not included in this abstract, the invariant branches of the inversely unstable fixed points ${}^1\mathrm{I}$ and ${}^2\mathrm{I}$ are depicted in the original, Figure 4.3.

2.3.3 Homoclinic orbits (complete sequences) represented by Figure 4

The α and ω branches in Fig. 4 are not drawn very long from the fixed point D as shown in the figures. However, the term α and ω branches originally represent half-line curves (of infinite length) in the phase plane in the time variable $t \in (-\infty, +\infty)$.

Based on the α and ω arcs in Fig. 4, it is essential to infer the infinite-length α and ω branches, and furthermore, to elucidate the motion of the representative points (of the discrete dynamical system) associated with these figures, especially their behavior at $t \to \pm\infty$.

Next, let us describe briefly, how the invariant branches and homoclinic points

[*7] The symbols that identify the infinite number of homoclinic points depicted by the numerical experiment are important for understanding the set of homoclinic points. Although the integers are suffixed, they represent the symbols that identify the "points (location) and the original integers (order)."

were given the names introduced so far (a detailed explanation is given in the original document, but the description is not organized in one place. The following intensive description, may be easier to understand).

It is not easy to visually track the motion of a homoclinic representative point (successive images of a discrete dynamical system) on a homoclinic structure. The fact that the representative points are on both the α branch and the ω branch is part of the complication. However, if the motion of the representative point is regarded as motion on the α branch up to a certain point and motion after that is regarded as motion on the ω branch, the above troublesome situation may be somewhat reduced.

The points where the α branch transfers to the ω branch are the cusp points marked in Fig. 4(a) and (b), i.e., the homoclinic points ${}^{\mathrm{A}}0_b$ and ${}^{\mathrm{B}}0_b$, in Figures 4(c) and 4(d), the points ${}^{\mathrm{C}}0_d$ and ${}^{\mathrm{D}}0_b$, respectively [*8]. Hereafter, the cusp points are sometimes called the interchange (homoclinic) points [*9].

It should be noted that the cusp points are not always marked with 0_b (the criteria for selecting the points will be described later).

The arc α (or, ω) with endpoints at any two points on the branch, say, points p_0 and p_1, is denoted by $\alpha(p_0, p_1)$, for example. The arc $\alpha(p_0, p_1)$ in the case where the two points p_0 and p_1 are not arbitrary two points and p_1 is the image of p_0 is called the unit time arc at point p_0 in the α branch (note that the ω branch is defined in the same way, but the ω branch extension is in the opposite time direction). If n is an integer and the point p_n is the image of n iterations of p_0, then the sum of the arcs $\alpha(p_n, p_{n+1})$ is an α branch. In other words, α

[*8] For the sake of clarity, the symbol D is omitted from Figs 4 (b) and (c) to indicate the directly unstable fixed point.

[*9] In the original, it was not called a cusp point or an interchange point, but a base homoclinic point. It is complicated to distinguish the infinite homoclinic points that appear in the experimental results. In writing this article, the author was forced to reconsider the terminology several times. Even at this point, it is difficult to say that we have reached a consensus.

The author realized that the notation "base homoclinic point" instead of "cusp point" used when writing this document is inappropriate because it is misleading as "beginning point of base interval 0_a".

In the original book and in the present document, various names are used to identify the homoclinic points depicted as the results of numerical experiments. However, there is no uniquely defined point other than the "nearest homoclinic point".

branches are marked with a scale.

The unit time arc of the α branch at point p_n converges to the fixed point D at $n \to -\infty$, while the unit time arc of the ω branch converges to the point D at $n \to +\infty$. Arc length converges to zero, and unit time arcs are aligned on eigenvectors in the neighborhood of the fixed point D when n is sufficiently large.

From here we move on to the description of Figure 4(a) and/or (b). We now describe how to take the cusp points (interchange homoclinic points) on the α_1, ω_1, and α_1, ω_2 branches and the base interval arc ($n = 0$). We focus on an arbitrary homoclinic point of α, ω branches and denote this point by h. The α and ω arcs connecting the fixed point D and the point h are uniquely defined. The sum of these arc lengths is defined as the (arc length) distance of the homoclinic point h from the fixed point D.

For any homoclinic structure of type A, B, C or D, there exists an homoclinic point with the minimum distance from the fixed point D. The homoclinic point with the smallest distance is called the nearest homoclinic point.

The unit time arc corresponding to the origin on the invariant branch (with $n = 0$) is called the base interval arc. The basic homoclinic points $0_a, 0_b, 1_a$ in Fig. 4(a) and the points $0_a, 0_b, 0_c, 0_d, 1_a$ in Fig. 4(b) were selected so that these unit time α arc and ω arc contain the nearest homoclinic points and interchange homoclinic points (cusp points).

Homoclinic points, all elements of complete sequences of $0_a, 0_b$ (or $0_a, 0_b$, $0_c, 0_d$) belonging to the base interval of $n = 0$ are called basic homoclinic points. The complete sequence of basic homoclinic points is on the basic homoclinic cycle, and of all the homoclinic points suggested by Fig. 4, the homoclinic points other than the basic homoclinic points are called derived homoclinic points. The complete sequence of derived homoclinic points has elements that deviate from the basic homoclinic cycle. In the original document, the derived homoclinic points are classified according to the number of deviant elements [*10].

[*10] A homoclinic complete sequence, which is a bi-directional infinite sequence, consists of 3 sub-sequences. The center is a finite point sequence and the front and back are (one-sided) infinite point sequences. A homoclinic complete sequence with a finite sequence of points in the center is a derived homoclinic sequence, and a homoclinic complete sequence without a finite sequence of points in the center is a basic homoclinic

The above items are summarized and the procedure for selecting the base interval arc is described below. First, the nearest homoclinic point is obtained. Next, the endpoints 0_a and 1_a of the base interval is selected so that the nearest homoclinic point and the interchange homoclinic point belong to the base interval. Although there is a degree of freedom in the selection of endpoints, it is preferable to take advantage of the symmetry between branches and/or to select a base interval where the α arc and ω arc do not intersect [*11].

Thus, the nearest homoclinic point, the interchange homoclinic point, the base interval homoclinic points, and the basic homoclinic points are determined, and it should be noted that the outlook of the description on the homoclinic structure changes remarkably depending on the selection of these points [*12].

Although there are various types of doubly asymptotic points on the invariant branch (to be described later), the number and distribution state of each type of points (the structure of the branch) are concentrated in a single unit time arc (e.g., the base interval at $n = 0$).

In closing this section, we would like to add that although the chaotic attractor UCA has many saddle-type periodic points in addition to the fixed points, the structure of the invariant branches of the periodic points is basically considered to be the same as those of the fixed points.

2.3.4 Homoclinic and periodic sets of UCA

There are infinitely many periodic points in the neighborhood of the homoclinic point, that is, the homoclinic point is an accumulation of periodic points (a well-known property of homoclinic points). Although we mentioned that there are infinitely many periodic points, the period becomes infinitely long as

---

sequence.

[*11] The symmetry of the α and ω branches is depicted in the portrait diagram of Eq.(1), which represents a conservative system with zero damping coefficient (see the original book, Fig. 4.6). The dissipative system described here is not a (strict) symmetry, but a rough outline symmetry.

[*12] In Fig. 4(a), the nearest homoclinic point is 1_a and the interchange homoclinic point is 0_b. Although the location of the nearest homoclinic point is fixed in both cases, the type B in Figure 4(b) or the type C in Figure 4(c), there is still some freedom in the way the symbols that identify the cusp and the base interval are assigned.

We encourage you to try various selections and comparisons, including whether or not the diagram in this document is the reasonable one.

one gets closer to the homoclinic point.

In this section, we first summarize the structure of the homoclinic points on the invariant branches of the fixed point D in Fig. 4(a). In the original, the number of intersections of $\alpha_1(0_b, 1_a)$ arc and ω_1 branch is counted by cutting unit time ω_1 arcs sequentially from the ω_1 branch. The number of intersections between the $\alpha_1(\,0_a, 0_b)$ arc and the ω_1 branch is also counted by the same procedure, and together with the above results, it is inferred that there are an uncountable infinite number of homoclinic points (type A) on the base interval arc $\alpha_1(0_a, 1_a)$ [*13].

Based on the fact that the homoclinic points shown in the Figure 4(a) are transversal, we hypothesize that the number of intersections of $\alpha_1(0_a, 1_a)$ arc and ω_1 branch is uncountably infinite and distributed densely on base interval arc, i.e., $\alpha_1(0_a, 1_a)$ [*14]. In addition, see also the equation (3.8) in the original

---

[*13] The intersection of the $\alpha_1(0_b, 1_a)$ arc and the arcs cut sequentially from the ω_1 branch is made according to the Cantor set composition rule (see the original, Figure 4.1).The situation is described as follows;

First step, the number of intersections with $\omega_1(-1_a)$ is 2,
Second step, the number of intersections with $\omega_1(-2_a)$ is 4,
Third step, the number of intersections with $\omega_1(-3_a)$ is 8,
...

Above, up to the four intersection points of the second stage are drawn in Figure 4(a), but note that in a drawing of this size, the shape of the $\omega_1(-2_a)$ arc indicates that this would be a barely discernible limit (no room between curves). Also, 8 of the third stage are not drawn (ω_1 branches have short drawn lengths; Details on these are shown in the original Figure 4.1). Note; $\omega_1(-n_a)$ is a simplified symbol for $\omega_1(-n_a, -n_b)$, where n is a natural number.

The endpoints of the α_1 arc corresponding to the central trisection are two derived homoclinic points belonging to the set $\alpha_1(0_b) \cap \omega_1(-1_a)$. Moreover, it should be noted that the number of clippings increases, the number of intersections exceeds the constitutive law. In other words, as the number of clippings increases, the number of intersections becomes larger than that depending on the Cantor set construction rule. This is because intersections are created even in the central trisection section that is clipped in the Cantor set construction rule.

[*14] (Key points regarding density or cardinal number considerations are briefly described so that the reader can follow the plot by filling in the gaps between the lines.)

The unit interval arc $\alpha_1(n_a, (n+1)_a)$ is denoted simply as the sum of two arcs $\alpha_1(n_a)$ and $\alpha_1(n_b)$. Similarly, $\omega_1(n_a, (n+1)_a)$ is denoted by $\omega_1(n_a)$ and $\omega_1(n_b)$, for simplicity. Note; Simplification symbols are only used between two adjacent points in the basic homoclinic point sequence.

The shape of the base interval arcs $\alpha_1(0_a), \alpha_1(0_b), \omega_1(0_a), \omega_1(0_b)$ and the description of $\alpha_1(-n_a), \alpha_1(-n_b), \omega_1(n_a), \omega_1(n_b)$ when n is sufficiently large are omitted.

for homoclinic points of type B on the arc $\alpha_1(0_a, 1_a)$.

The confidence in the existence of true contacts in the neighborhood of the contacts seen in Figures 4(b) and 4(c) was further increased by drawing invariant braches for the perturbed systems with the constants slightly shifted on both sides from the representative UCA values (see Figs. 5.1 - 5.4 in the original).

By summarizing the fact that α branch of the directly unstable fixed point D is asymptotic to itself (the normal section is a complete set), and ω branch is distributed in a Peano-curvilinear manner, we have derived the hypothesis that in addition to transverse homoclinic points, singular (non-transverse) homoclinic points are always present on the invariant branches of the directly unstable fixed point D.

Next, let us discuss periodic points on the UCA. The set of all periodic points on the UCA is called the periodic set. Needless to say, periodic set is not on the α branches and belongs to the ω limit set of the α branches. In the original document, it is hypothesized that periodic points, like homoclinicpoints, have uncountable infinite density and are distributed densely everywhere in the UCA.

There are three fixed points as periodic points with the smallest period (these are described in 2.3.1). The invariant branches of the directly unstable fixed point D is depicted in Figure 4; see also, Figure 5 below for a superposition of the four panels of Figure 4(a) - 4(d). In the original, typical examples of 2-periodic and 3-periodic invariant branches are depicted. On the basis of these, we deduce the outline of the shape of the invariant branches at the n-periodic points (see the next section).

In connection with the above, when n is sufficiently large, the endpoint neighborhoods of $\alpha_1(n_a)$ and $\alpha_1(n_b)$ are parallel to the α_1 branch root in the neighborhood of point D. The appearance of the arcs $\omega_1(-n_a)$ and $\omega_1(-n_b)$ is similar to the above.

If we apply n iterative inverse mapping to the intersection of the arc $\alpha_1(n_b)$ and the ω_1 branch, the image is a homoclinic point on the basic interval arc $\alpha_1(0_b)$.

Let's assume an α_1 arc with no homoclinic points (the length of the arc is not zero) on the α_1 branch (or on the base α_1 interval). How small (or short) the α_1 arc is, the image by its iterated mapping can be as long as possible, and this image does not extend beyond the UCA, and its approximate shape may be guessed from the UCA.

Since almost all the homoclinic points seen in Figure 4(a) are transversal, we can see that it is impossible for this stretched α_1 arc not to intersect with the ω_1 branches (see not only Figure 4 but also Figure 5 and 6). Further explanation is probably not necessary.

The original book defines UCA as a closure of α_1 and α_2 branches. The description of heteroclinic points (set) is omitted, but it should be noted that heteroclinic point and homoclinic point in the chaotic attractor UCA are the accumulation points of each other's partner sets [*15].

2.3.5 UCA depiction on a phase plane

In this section, the author would like to describe the "shape, form, or being" of the chaotic attractor represented by the Duffing equation (1), using his imagination as well as all the matters that he has experienced so far. Because of these circumstances, it is inevitable to include in the description some matters that are difficult to follow up academically or technically. He would like to caution you in advance.

The simplest chaotic attractor known to the author, represented by the Duffing's equation, is reported in Figures 2 and 3 of Ref. [1] [*16]. The simplest reason is that there is only one element with the shortest period in the periodic set, and its α branch is not asymptotic to any fixed point other than its own root fixed point (i.e., the ω limit set of the α branch of the inversely unstable fixed point contains no fixed points other than its own root).

Such a chaotic attractor is henceforth referred to as the prototype attractor. At the beginning of this study, this attractor was once considered as a subject for numerical experiments, but was not adopted. The reasons are that the chaotic attractor is too thin (the details are difficult to be drawn because the invariant branches almost overlap each other due to the large damping coefficient), and the shape of the attractor is too simple. We have not encountered a chaotic attractor that retains the structure of the prototype and is inflated (with a small damping coefficient).

From here we return to the description of the UCA system (1). At first glance,

---

[*15] Let n and m be arbitrary natural numbers and l be one of the common multiples of n and m. The heteroclinic point connecting n-periodic points and m-periodic points of UCA is expected to be an accumulation point of homoclinic points of l-periodic point (conjecture).

[*16] The Duffing equation in this example differs slightly from equation (1) in which the external force term contains a DC component ($B\cos t + B_0$). It is an attractor that appears when the constant (k, B, B_0) value of the system is $(0.2, 0.3, 0.08)$, has one fixed point, and is inversely unstable.

both ^{1}I and ^{2}I, the two inversely unstable fixed points in the UCA, appear to be root fixed points of the α branch, which is similar to the prototypical chaotic attractor. However, since the extended α branches behave as if they span the whole UCA, each of them is not an (isolated) attractor (see the original, Fig. 4.3).

The fixed point ^{1}I (or, ^{2}I) and its α branch is an invariant set (curve) of period 2 if we focus on only one α branch leaving the fixed point. However, if we consider the two opposite α branches at the fixed point as a single connected curve, then an invariant set of period 1 (see the context).

At the first glance, the α_1 and α_2 branches of the directly unstable fixed point D seem to enclose and fold the α branches of the inversely unstable fixed points ^{1}I and ^{2}I, respectively (see original, Figures 3.7 and 4.2). That is, the α branches of fixed points ^{1}I and ^{2}I are contained in the ω limit set of the α branches of the directly unstable fixed point D [*17].

In the original, we consider 3-periodic points in UCA. There, the existence of period-3 skeleton set in UCA is suggested (see the original, Figs.3.8 (b) and 4.5). These 3-periodic skeleton sets are embedded in the gaps without overlapping with the skeleton set of period-1 (3-periodic skeleton set, 9-periodic skeleton set following the 3-periodic skeleton set, etc., are interesting but not included). Furthermore, the 3-periodic α branches other than the skeleton set encompass all the central points and are membranes of the UCA (see Fig. 4.4 in the original book).

Thus, it is no exaggeration to say that the main shape and structure of the UCA are dominated by the $\alpha\,(\alpha_1, \alpha_2)$ branches of the fixed point D.

The next major α branches after the 1-periodic α branches of the fixed point D are the 3-periodic α branches. The 3-periodic α branches form the 3-periodic skeleton sets or the membraranes of UCA.

Moreover, we feel that the actualities of m-periodic α branches (where m is

[*17] Considering that all these branches, the $\alpha\,(\alpha_1, \alpha_2)$ branch of D and the α branches of ^{1}I and ^{2}I, are of infinite length, is it appropriate to represent one as enclosing the other? In fact, the author doesn't know how to describe it.

He feels that among the many periodic branches, the 2- and 3-periodic α branches exhibit a behavior that does not conform obediently to the invariant branch at the ifixed point D.

any natural number ($\neq$ 1, 2, 3)) are embeded in the gaps between the 1-, 2- and 3-periodic α branches, and will not have any influence on the shape of UCA [*18].

2.4 Decomposition of UCA

UCA is a set of central points, and this set is asymptotically stable. The central point is a recurrent point or an accumulation point of recurrent points. UCA can also be expressed as UCA is composed of a minimal set and a set of central points that are not recurrent points.

A minimal set is the smallest unit that represents a theoretical steady state and is an invariant closed set with respect to the transformation (mapping) T. The periodic group and the quasi-periodic group are well-known minimal sets [*19].

The central point, which is not a recurrent point, is the intersection of the invariant branches of the periodic points and is called the doubly asymptotic point. In addition to the well-known homo- and hetero-clinic points, the original book introduced chaos-clinic points (assuming the existence of saddle-type recurrent points).

At the risk of disrupting the flow of the discussion, we would like to mention chaos-clinic points here. Chaotic phenomena (time series) represented by computers have presented us with various outstanding properties. The sensitive dependence on initial conditions, predictability in a short period of time, and unpredictability in a long period of time are typical examples. The chaotic

[*18] Let us call the periodic point that produces the membrane the outer boundary periodic point. In the case of UCA, there are 3-periodic points, which may be due to the fact that the Duffing equation (1) is expressed in terms of a third-order nonlinear characteristic. We expect that the shape of the nonlinear characteristic curve (order and symmetry of the curve) determines the period and properties of the outer boundary periodic points. In addition to the above, there is an unexplored matter of concern. It is the relationship between "the UCA covering is 3-periodic" and "the period 3 that made Li and Yorke famous". The author feels that there may be a significant relationship between the three periods of the basis of chaos $x_{t+1} = ax_t(1-x_t)$ and the three periods of the UCA membrane, which has not yet been noticed by anyone.

[*19] Quasi-periodic groups do not exist in the dissipative UCA system (1). The minimal set whose existence or non-existence is unknown is sometimes called the third minimal set instead of chaotic minimal set. The chaotic attractor obtained by numerical experiments strongly suggests the existence of chaotic minimal set (covering the entire attractor region). Note, however, that (theoretical) chaotic minimal sets, if exist, represent deterministic time series and do not exhibit randomness or stochastic behavior.

attractor, which corresponds to the orbit or trajectory of chaotic phenomena, presents a difficult problem regarding the structure of the exact solution that gives rise to the chaotic attractor.

In general, steady-state phenomena of nonlinear systems are represented by minimal sets. For example, when the exact solution for the UCA in Figure 1 is discussed, the first step is to find a minimal set solution that is asymptotic to the entire computer UCA-wide (for a moment, let us close our eyes to the appearance of irregularities). This minimal set is called a chaotic minimal set in the original paper.

What has been stated so far in the text is that the UCA contains an infinite number of periodic solutions (minimal sets). This may be sufficient to explain the actual phenomenon, but the fact that there is no chaotic minimal set (non UCA-wide) is left unexplained. The chaos-clinic point on the α branch is the initial value that converges to the chaotic minimal set, as the recurrent point is assumed to be saddle-type.

There may be a chaotic minimal set among the infinite number of minimal sets contained in the UCA in Figure 1. It seems to be extremely difficult to deny the supposed matter (the author may have set up a sterile problem and fallen into a pit he dug himself).

From here, we get back to the story. The α branch of any fixed or periodic point on the UCA contains no points other than the doubly asymptotic points mentioned above. The periodic points and (possibly existing) recurrent points of the UCA belong to the derived set of α branches.

The set of all central points marked on the phase plane is (theoretical) UCA, but the complete sequence of any initial value (a point p outside chaotic minimal set) on UCA is only a subset of UCA. We shall describe the details somewhat more carefully in the following.

The point p on the periodic set yields (immediately without any transient behavior) a periodic motion. Similarly, a point p on a third minimal set represents (immediately) deterministic chaotic motion (the complete sequence in this case is non-UCA-wide, and the corresponding time series shows no irregularity).

The set of central points other than the recurrent point, i.e., the points p on the α branches, go through a transient behavior and asymptotically approach

periodic motion or deterministic chaotic motion. Note, however, that the existence of an infinite number of periodic points in the neighborhood of point p on the α branch is a distinguishing feature.

This property implies the inevitability of recurrence in the observed positive half sequences in relation to the real phenomena. In other words, the exact theoretical solution converges to periodic motion through transient state, while the real phenomenon is observed as stochastic recurrent motion — this feature is the indescribable strangeness of the chaotic attractor, and the designation "central point" seems to be an appropriate one [*20].

The above can be summarized as follows:

In theory, the ω limit set of any point p in the UCA is a periodic or chaotic minimal set. In reality, it is a transitional phenomena that continues to wander chaotically throughout the UCA for all points p. The author called these phenomena "chaotically transitional phenomena" (the title of the original book).

The α limit set of any point p in the UCA is a periodic or chaotic minimal set. The realization is "divergence to infinity" for all points p.

The decomposition of UCA can also be expressed as follows.

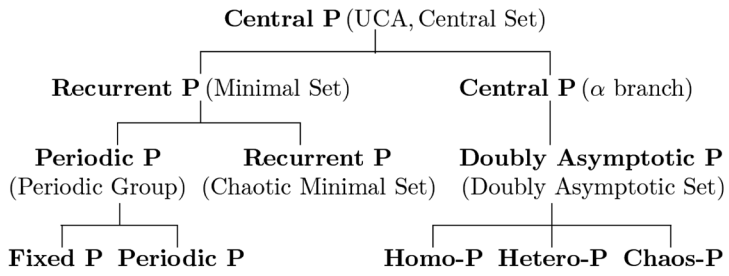

Diagrammatic representation of the decompositin of UCA

2.5 Concluding Remarks of this Chapter [*21]

[*20] This property (structure) seems to mix the effects of "disturbance to which the representative point is subjected" and "fluctuation to which the system is subjected" on the phenomenon. In other words, in analog experiments, the two are indistinguishable, but in digital experiments, the latter irregularity does not appear (unless the irregularity is taken into account at the programming stage).

[*21] This section is a summary of the main results (not included in the discussion at the time of writing the original document). It is written with reference to Figures 5 and 6, but does not necessarily need to be read after Chapter 3.

The above description and the view on the details of the set of central points on the disk described below are considered to be extremely important for understanding the nature of the chaotic attractor. This view is described as "For any fixed or periodic point on the UCA, there is a set of initial points that leads to (converges to) this point, and the initial points are densely distributed throughout the attractor (of course, theoretical hypothesis)". In other words, any given disk may be described as containing initial values that asymptotically approach an arbitrary fixed or periodic point in the UCA [*22].

This view is a summary (aggregation) of examinations based on the results of numerical experiments described in the original book. Although the author has described it above as a hypothesis, he cannot deny that he has some misgivings if he ask himself whether it has been sufficiently verified (overinterpretation of experimental results, entrenchment of unconscious imagination, lax theoretical considerations, etc.). It is indisputable that this is an issue that should be addressed with caution, since the content is the very basis of the chaotic phenomena. Therefore, please understand that this is a hypothesis whose credibility and robustness must be questioned.

The following is a list of the main points that form the core of the above discussion, but please refer to the text or the original document for the details of the experimental results and the process of their consideration (the following description is a repetition of the previous description).

In Figure 1, the UCA is represented by stroboscopic observation points (disks, circles of non-zero radius). These are the experimental results themselves, but the disks on the theoretical UCA represent the neighborhoods (open sets) of the representative points (of the discrete dynamical system).

The UCA is defined as a closure of α_1 and α_2 branches of a directly unstable

[*22] This property was already well known at the beginning of the discussion of chaotic phenomena. The author had no objection to its observation in phenomena observed experimentally (with transitions between minimal sets). However, it was not clear whether it was theoretically established (for exact solutions) or from the structural viewpoint of global solutions on the phase plane.

At this point in time, it would not be surprising if the theory has been proven. The author is aware that he is not familiar with the actual situation in this field, so if the discussion has already ended, please let inform him. Nor does he believe that his presentation of the results of the experiment described here is the end of the story.

fixed point D. These branches are infinitely folded, fractally stacked curves of infinite length.

The ω_1 and ω_2 branches of the fixed point D and the $\alpha(\alpha_1, \alpha_2)$ branch above are also called invariant branches of the fixed point D. The set of all homoclinic points that the invariant branches constitute is called the homoclinic set that the fixed point D constitutes (simply, the homoclinic set of point D). The homoclinic set of the point D is uncountable in density and is densely distributed all over the α branch of the point D.

The $\omega\,(\omega_1, \omega_2)$ branch at the point D is conjectured to fill the UCA's basin (phase plane) in a Peano-curved form (the root portions of the ω_1 and ω_2 branches are depicted in Figure 5)

There are an infinite number of periodic points as well as fixed points on the UCA. Each periodic point in the derived set of $\alpha\,(\alpha_1, \alpha_2)$ branch has a doubly asymptotic structure [*23]. The periodic set of the UCA (the set of all periodic points) is uncountable and is distributed densely on the UCA.

We would like to remind you of the "outer boundary 3 periodic points". The 3-periodic α brancehs of this 3-periodic points constitute the UCA membrane (see Figure 4.4 in the original book).

Correspondingly, from the 3-periodic points U, V, and W, there is no central point on the ω branch away from the UCA (left or lower left), but the ω branch toward the opposite side is inferred that behaves Peano curve-like behavior (see Figure 4.5 in the original).

However, all ω branches in both directions except the above 3-period branches are loaded with central points and behave like Peano curves, just like the $\omega(\omega_1, \omega_2)$ branch at the fixed point D.

The neighborhood (disk) of any central point on the UCA contains a fractally stacked, uncountable infinite number of α arcs. The whole of these α arcs lies on an infinitely long, infinitely folded α branches of fixed and periodic points.

There are many α arcs in the disk containing a single periodic point, but even if there are α arcs that do not carry a periodic point, the periodic point is

[*23] The UCA is defined as an invariant set under a mapping (one transformation T). The $n(\neq 1)$-periodic points and n-periodic α branches are contained in the derived set of $\alpha(\alpha_1, \alpha_2)$ branches. When considering the time evolution of a periodic point or periodic branch, note the number of iterations of the iterated map.

outside the disk. Also, points that differ from the the doubly asymptotic points on the ω branches are wandering points.

Let us focus on an arbitrary periodic point on the UCA and assume that this periodic point is marked on Figure 5 (and/or 6), which depicts the ω branches of the fixed point D. The ω branch at this periodic point has to be extended along the ω branches of Figure 5 (and/or 6), with a gap between the ω branches at point D.

The hypotheses derived from a summary and discussion of the above matters are highlighted at the beginning of this section.

3. Substantial stability and bifurcation phenomena of UCA

This Chapter is a summary of Chapters 5 and 6 of the original book.

A structurally stable system is described as follows. Consider a set of perturbed system equations whose representative element is the ordinary differential equation we are interested in, and the global structure of the solutions of all equations belonging to this set is qualitatively the same [*24].

Andronov and Pontryagin proposed the following necessary and sufficient conditions for a system to be structurally stable:

1) there are no higher-order fixed or periodic points,

2) the α and ω branches of the saddle-type fixed and/or periodic points do not overlap (coincide with) or are tangent to each other.

Since then, this view has been interpreted as if it were the (original) definition of structural stability [*25].

However, considering the structural stability of the UCA system in the above sense, it is judged to be structurally unstable, since special-type doubly asymptotic points always exist in the system.

[*24] "How to set up a set of perturbed systems" and "How to determine that the global structure of the solutions is qualitatively the same" are major problems, but they seem to be open questions.

[*25] At some meeting, when the author stated that the chaotic attractor is represented by a closure of the α branch and that there are always homoclinic points of special type on the α branch, the reaction of not a few audience members was, "Are you talking about structural stability?" (This sentence describes the author's impression at that time in his own words) .

From this experience, the term "substantial stability" instead of structural stability was coined, but the author considers it a useless term.

Furthermore, the fact that chaotic phenomena have been observed and reported not only in the UCA system but also in many other real systems, we must conclude that the experimentally observed chaotic attractors have structural stability in the original sense.

This may depend on the following circumstances. The necessary and sufficient condition derived by Andronov and Pontryagin is discussed for 2-dimensional autonomous systems. Nevertheless, the reason for the discrepancy may be that we have easily expanded to 2-dimensional nonautonomous periodic systems.

The author may be the only one who misunderstands. However, it is thanks to this misunderstanding that he was able to get involved in this kind of numerical experiment.

Although we have made some superfluous descriptions, we will now turn to the main topic: the phase portrait diagram (the result of numerical experiments), which provides the supporting evidence that special-type homoclinic points are always exist in the UCA system and that the ω branch behaves like a Peano curve (filling up the phase plane).

Fig. 5 Prototypical homoclinic structure of UCA system

The invariant branches in Figures 4 are depicted as homoclinic structures of type A, B, C, and D, individually, and Figure 5 is a superposition of these structures [*26]. By comparing with the omitted perturbation system diagrams

[*26] Figure 5 depicts useful information that contributes to understanding the basic structure of chaotic attractors as well as the interrelationships among A-, B-, C-, and D-type homoclinic structures depicted in Figure 4 earlier. In this footnote, we will attempt to provide a specific and detailed description of the invariant branch geometry, with the intention of deepening your understanding of it (we will not touch on comparisons with perturbed systems, which are not included in this excerpt).

Specifically, in Figures 4(a) and 5, for example, we would like you to grasp the shapes of α-arc $\alpha_1({}^{\mathrm{A}}2_b)$ – simplified representation of $\alpha_1({}^{\mathrm{A}}2_b,{}^{\mathrm{A}}3_a)$ –, and ω-arcs $\omega_1(-{}^{\mathrm{A}}2_a)$, $\omega_1(-{}^{\mathrm{A}}3_b)$, etc.

Once these are solved, the following will be nodded easily. The number of intersection points of the $\alpha_1({}^{\mathrm{A}}0_b)$ arc and the ω_1 branch mentioned in the original book:

The number of type A homoclinic points on the $\alpha_1({}^{\mathrm{A}}0_b)$ is produced by the ω_1 arc series $\omega_1(-{}^{\mathrm{A}}n_a)$ –where n is the natural number – following Cantor's rule at the initial stage (n is small), whereas the series $\omega_1(-{}^{\mathrm{A}}n_b)$, although not following Cantor's rule rigidly, would not be totally irrelevant for the production of type A homoclinic points. Moreover, the shape of $\omega_1(-{}^{\mathrm{A}}n_a)$ in the former series can be predicted to some extent, but those $\omega_1(-{}^{\mathrm{A}}n_b)$ in the latter series are difficult to predict.

(original, Figures 5.6 and 5.7), many insights, such as the tendency of the invariant branches to transform as the damping coefficient increases or decreases, may be obtained.

Fig. 6 Evidence of the existence of special-type d.a. points on UCA

Also, even if the α branches of all periodic points in the UCA are infinitely lengthened, they do not extend beyond the UCA in the figure along with its ω limit set.

In the phase portrait, the infinitely layered α branches of all periodic points are replaced by the observed UCA in Figure 6. In this figure, we can infer the existence of special-type doubly asymptotic points from the shape of the invariant branches in the following manner.

In Figure 6, let us look for the ranges where the gradients of the α branches of all periodic points (on UCA) are equal to the gradients of the ω_1 and ω_2 branches [*27].

In more than a few places (not marked in the Figure 6 because important information would be lost if it were marked), we can find contact points between bundles of α branches and $\omega\,(\omega_1, \omega_2)$ branches. Moreover, these contacts seem to be distributed on certain curves.

The author is convinced that "true contacts" exist in the neighborhood of such contacts. Furthermore, even if the true contact point disappears with a change in the constant value of the system, a new true contact point still appears. Needless to say, the true points of contact are the higher-order homo- or hetero-clinic points between the elements in the periodic set of UCA [*28].

Also, as the series $\omega_1(-^{\mathrm{A}}n_a)$ advances (as n increases), the number of intersections calculated will be larger than in Cantor's rule. Moreover, you can see that the excess intersections appear in the interval corresponding to the central trisecting interval, which is eliminated by Cantor's rule.

[*27] We would like to ask you to make a bold guess, bearing in mind that the ω branch is drawn short and the blank space is wide, but the extension of the ω branch is a Peano curve.

Note that the extension of the ω branch beyond the illustration of the ω branch drawn in Figure 6 would be difficult on a computer with a 64-bit real number representation.

[*28] The following footnote is a reminder for a deeper understanding of the ω branch in Figure 6.

Depicted as ω branches in Figure 6 are two arcs $\omega_1(-^{\mathrm{A}}4_a, \mathrm{D})$ and $\omega_2(-^{\mathrm{D}}4_a, \mathrm{D})$. Just

From the ω branches in Figure 6, it is difficult to imagine an infinite extension of the branches. However, based on the supporting evidence such as the dense distribution of homoclinic points on the α_1, α_2 branches of the fixed point D, the following hypothesis is derived [*29]. That is, the ω branches will fill the phase plane in the form of Peano curves. If noted carefully, in general, the region filled by the ω branches is usually the basin of the attractor, not the entire phase plane.

The above concludes the description of substantial stability, but the original book shows a phase portrait diagram of a perturbed system with the following three constant values of $k = 0.055, 0.050, 0.045$, $(B = 7.5)$. The fact that the experimental results are built-in must be described through the subjectivity of the viewer (see the original, Figures 5.2, 5.3, 5.6, and 5.7).

Next, we discuss the bifurcation phenomena of UCA. Deterministic phenomenon is represented by a single isolated, asymptotically stable minimal set. However, it is not uncommon to find an infinite number of unstable minimal sets hidden in the phase plane of the system representing the deterministic phenomenon (and the entire phase plane is the basin of the deterministic attractor). This describes the phase portrait of the window phenomenon (i.e., system constant value in the window) found in the chaotic region [*30].

---

as we saw the shape of the invariant branches in Figure 5, let's get specific about the shape of the ω branches (arcs) depicted in Figure 6.

First, we would like to ask you to identify the arc $\omega_1(-^{\mathrm{A}}3_b)$ in Figure 6. It is not easy to signalize it, but if we denote by $\pi(-^{\mathrm{A}}3_b)$ the region enclosed by the simple closed curve represented by $\omega_1(-^{\mathrm{A}}3_b)$ and $\alpha_1(-^{\mathrm{A}}3_b)$, for example, it is easy to draw a diagonal line in this region. (The answer is to identify the corresponding region depicted in Figure 5 and bring the shaded region into Figure 6.)

Next, we would like you to shaded the arc $\omega_2(-^{\mathrm{D}}3_a)$, that is, $\pi(-^{\mathrm{D}}3_a)$ (the answer is not drawn in Figure 5, but in Figure 6. This is difficult, so please read Section 4.2 after you understand $\pi(^{\mathrm{D}}0_a)$, $\pi(-^{\mathrm{D}}1_a)$, and $\pi(-^{\mathrm{D}}2_a)$ depicted in Figure 4(d)).

The arcs $\omega_1(-^{\mathrm{A}}4_b)$ and $\omega_2(-^{\mathrm{D}}4_a)$ are images from the inverse mapping of $\omega_1(-^{\mathrm{A}}3_b)$ and $\omega_2(-^{\mathrm{D}}3_a)$ seen above. At first glance, the differences from the original images $(n = 3)$ are so pronounced that it would be impossible to even imagine the approximate shape without the aid of a computer.

[*29] Another collateral evidence is related to the bifurcation phenomena below.

[*30] A concrete example is a perturbed UCA system with constants $k = 0.05$, $B = 6.70$, $6.71, 6.72$. In this system, there is a 5-periodic point attractor and a transparent UCA in its basin. The deterministic 5-periodic attractor and its basin wedged in the pre-branch central point set, but all elements of the pre-branch central point set remain.

The original draws a phase portrait diagram in which the UCA instantly vanishes and a fixed point attractor appears ($k = 0.05, B = 8.5$). Although there is a problem in calling the bifurcation there a window phenomenon, I-type fixed point in the UCA is transitioning to an S-type fixed point by emitting two D type 2-periodic points [*31]. At the bifurcation point, there exists a higher-order fixed point, which is a merger of an I-type fixed point and two D-type 2-periodic points (three in total). This IS-bifurcation is a global bifurcation with no hysteresis property.

The attractor UCA instantly disappears as soon as it passes through the bifurcation point, but the set of central points in the UCA (just before the bifurcation) remains in the perturbed system after the bifurcation. In other words, this bifurcation is caused by the loss of attractiveness of the central point set. These sets of central points that have not been erased but have lost their attractiveness are called "transparency UCA".

In the 5-periodic window phenomenon mentioned in the original text, the I-type 5-periodic points go through a similar bifurcation to the S-type 5-periodic points, and on the other side of the window, they return to the chaotic state through a cascade of rapidly evolving period doubling bifurcations [*32].

The original book also draws a phase portrait of the case where the UCA is

---

[*31] The UCA system in question has two S-type fixed points. Each of the real basins is observed as two narrow domains of attraction containing two fixed points. For example, assume the situation where ω branches are added to the inversely unstable fixed points (two white squares) in Figure 5, and these ω branches are widened from lines to bands. The widening is done by slightly widening the area near the squares and narrowing it as we move away from the squares. Thus obtained is a portrait diagram of these squares replaced by the stable fixed points ^{1}S, ^{2}S. Outside of those basins, it is not determined which of the two basins is the real one.

This is due to the fact that the ω branch representing the basin boundary is swallowed by the doubly asymptotic structure inside the transparent UCA. Their entanglement can be inferred to some extent from the ω branches at the inversely unstable fixed points ^{1}I and ^{2}I just before the bifurcation (see Figures 6.4 and 6.6 in the original article).

[*32] The IS-bifurcation phenomenon described above, in which the UCA transitions to the fixed point attractor, is not called a window phenomenon because it does not return to the chaotic state even if the constant B of the system is continuously increased. However, the IS-bifurcation described here is the bifurcation on one side (window opening) of the window phenomenon that appears in the chaotic region, while the other side (window closing) is a cascade of rapidly evolving period-doubling bifurcations that revive the transparent central point set.

extinguished by contacting ω branches of 2-periodic points (these are located outside of UCA). In this case, the transparent UCA still exists [*33].

This is the extent of our introduction to the transparency metamorphosis of UCA.

4. Supplementary notes

4.1 Reliability of Figures

The title of the article should be taken as "How accurate are the figures in this paper?" The figures depict the results of numerical experiments using a computer, and although the accuracy of the numerical analysis seems to be discussed, the accuracy is not verified. For example, the basic homoclinic points of the representative UCA system are approximations based on the author's comprehensive judgment based on his own experiences.

Let us consider (real or computer) fixed points for ordinary differential equations that are converged by iterative calculations to e.g. completely stable fixed points. Apart from this, let us assume (strict) fixed points based on a theoretically guaranteed arithmetic method. These real and strict fixed points are usually separated by a small distance. The distance between them depends on the numerical solution of the differential equations and the constant value of the method employed, but these are not verified in this article. Based on the above, please refer to the figures in this document.

There may be a slight discrepancy between the positions of these real and exact disks. However, the structure of the solution in both regions is considered to be qualitatively the same (the structure in the exact disk is inferred, or frankly speaking, left unexplained). This is the author's criterion or limitation.

[*33] The UCA contacts the ω branches of the 2-periodic points and vanishes, but the representative point settles at the asymptotically stable 2-periodic point attractor to which it jumps. The UCA system described here has two 2-periodic groups (attractors). The results of the grid method for the real basins of these 2-periodic group attractors show that the basin of any attractor is narrow, and the destination of the motion (any attractor) from the initial point given outside these real basins can be determined only stochastically (see Fig. 6.5 in the original paper).

The grid method phase portrait diagram described here is a corroboration of the hypotheses about the ω branch of the directly unstable fixed point D in the UCA (Peano curvilinearly), and the dense distribution of the doubly asymptotic set on the α branch of the point D.

We hope that you will take these considerations into account as you read this document. In other words, "This is the author's Rupert Sheldrake, Terence McKenna, and Ralph Abraham (1998)".

4.2 Supplementary explanation for Figures 5 and 6

The shapes of the arcs comprising the ω branches depicted in Figures 5 and 6 are described below. As mentioned earlier, we may substitute by describing the area enclosed by the ω and α arcs.

The arc $\omega_1(-^{\mathrm{A}}3_b)$ is depicted at the top of Figure 4(a), below. The region $\pi(-^{\mathrm{A}}3_b)$ undulates clockwise from the top of the figure to reach the root of the α_1 branch from the upper left.

The $\omega_2(-^{\mathrm{D}}2_a)$ is depicted in the left center of Figure 4(d), below. The region $\pi(-^{\mathrm{D}}2_a)$ reaches the root of the α_2 branch from the lower right clockwise from the left part of the figure.

The end of $\pi(-^{\mathrm{D}}3_a)$ is at the top of Figure 6 (slightly left of center, square shape with a protruding helmet on top). This elongated region descends clockwise in a semicircle, undulates and bends at the bottom, then turns upward (to the right of the narrow region that has just descended) in a semicircle, makes a clockwise U-turn at the upper right edge of the figure, followed by a clockwise descent at the right edge of the figure. This area can be easily identified in Figure 6. The $\pi(-^{\mathrm{D}}3_a)$ in the ahead is undulating along the ω_1 branch (the upper part of Figure 4(a) is easy to see) and reaches the root of the α_2 branch from the lower right.

Although it is difficult (or even impossible) to describe the shape of the curves in text, it is possible to trace the curves in Figure 6 to some extent. In Figure 6, the contact between the multiple curves is not very interesting to track, but since they do not intersect, the order before and after the contact is preserved (the ω branch shown in the figure is the $\omega\,(\omega_1, \omega_2)$ branch connecting the two homoclinic points $-^{\mathrm{D}}4_a$ and $-^{\mathrm{A}}4_b$ in a single stroke that does not intersect). Why don't you try to verify the above depiction by taking advantage of electronic publication and enlarging the figure?

Let's look at two edges of the elongated regions seen on the left edge of Figure 5. The top is the end of $\pi(-^{\mathrm{A}}3_b)$ and the bottom is the end of $\pi(-^{\mathrm{D}}2_a)$. These ends are bounded on the left side of Figure 6 by $\pi(-^{\mathrm{D}}4_a)$ and $\pi(-^{\mathrm{A}}4_b)$,

respectively. The bearded region seen in the lower part of Figure 6, the left side is the edge of $\pi(-^{\mathrm{D}}4_a)$ and the right side is the edge of $\pi(-^{\mathrm{A}}4_b)$. We may dispense with further explanation.

4.3 Differences between the original and the abridged translation

Since the original book was published last year, the author felt little progress in the contents of this abridged translation when he finished the first draft. It is true that the data seems to be correct, but as he worked on it, he felt the entire contents of the book slowly permeating his brain. This is how he arrived at the summary (hypothesis) described in Section 2.5. This is the result of having accepted the English translation.

One more note should be made regarding the existence or non-existence of a chaotic minimai set. This is a topic that carries considerable weight in the flow of this document, but it is easy to understand that there is in fact no UCA-wide chaotic minimai set. Since this has been an issue that has plagued the author for many years, the author has dared to use a description that preserves the flow of the original work. The previous descriptions of the chaotic minimai set and set of chaos-clinic points should be understood as the empty set ϕ. However, the existence of a third minimal set that does not extend over the entire area remains unresolved.

Finally, as a reminder, we would like to rewrite the summary of the structure of the UCA: The chaotic attractor UCA is a closure of $\alpha(\alpha_1, \alpha_2)$ branches of the directly unstable fixed point D.

The set of all fixed and periodic points belonging to the UCA and the set of α branches of all fixed and periodic points are the periodic set P of the UCA and the α (branch) set of the UCA. This α set is the set of doubly asymptotic points (d.a set) composed of all fixed and periodic points.

UCA is the sum of the set P, the d.a. set, and a third minimal set whose existence is unknown. The sets P and d.a. include higher-order periodic points and d.a. points of a special type, but their details and the relationship with the third minimal set have not yet been clarified — The recurrent point of the third minimal set may be higher order (assuming it is not saddle-type).

A further change in the flow of the discussion is the description of the expanded interpretation of the conditions established by Andronov and Pontrya-

gin (main text, 3.1).

New terms, such as interchange homoclinic point and disk, are introduced. Also added are details about the geometry of the invariant branches depicted in Figures 5 and 6. These are described as if they were exercises found in a normal introductory book. When the original book was written, we had considered including exercises, especially at the end of Chapter 2, but we realized that the readership of the original book (and this excerpt) is limited to specialists in nonlinear problems and theory of dynamical systems, so we decided that it was unnecessary.

The shape of the invariant branches in Figures 5 and 6, particularly the ω branch bending and folding situation, suggests that the ω branch will be repeated as the ω branch is extended, lending credence to the Peano-curved shape that would fill the phase plane.

It has been known for a long time that "the doubly asymptic points connecting any two periodic points of the UCA are densely distributed throughout the UCA," or "the neighborhood of any central point contains a doubly asymptotic point such that any two periodic points are α- and ω-limit points. But the author felt that these were a rule of thumb based on (inconclusive and unconvincing) observations.

However, during the writing of this English abstract, the author realized that Figures 5 and 6 may be illustrating concrete examples from the viewpoint of rigorous solutions. Although the authenticity of this statement requires further investigation, we would like to record it as an inference based on our experimental results.

5. Figures of the abridged abstract of the monograph "Theory of Chaotically Transitional Phenomena"

In this document, all figures drawn on the phase plane are the results of numerical experiments performed on equation (1). Details of the numerical solution methods used in the numerical experiments are omitted. The unit length ratio of the horizontal axis to the vertical axis is set to 5:1 in all figures, although the details of the figure display (e.g., drawing range) differ from figure to figure.

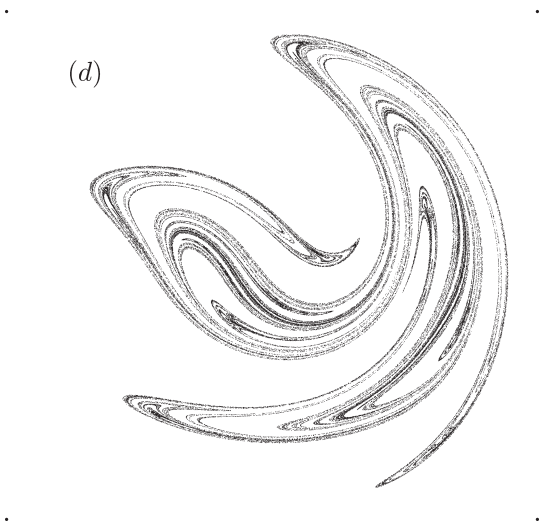

Figure 1. Chaotic attractor UCA

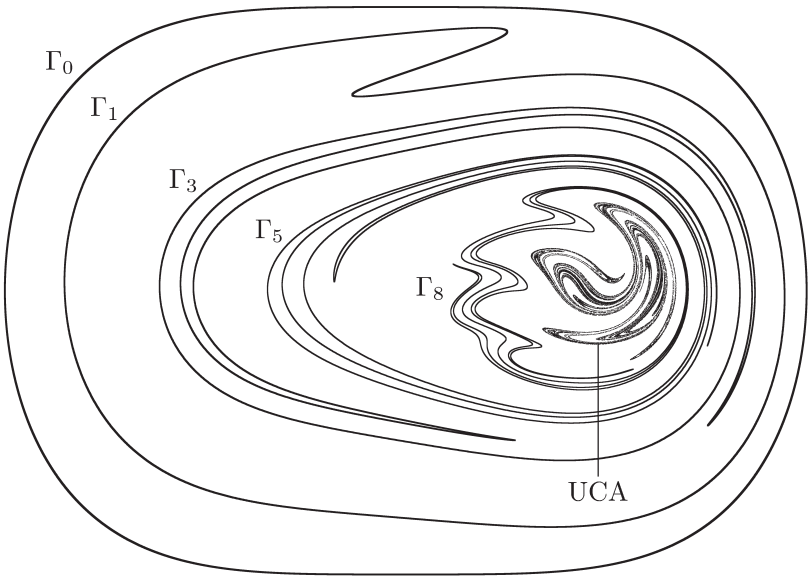

Figure 2. Maximum finite invariant set of UCA system

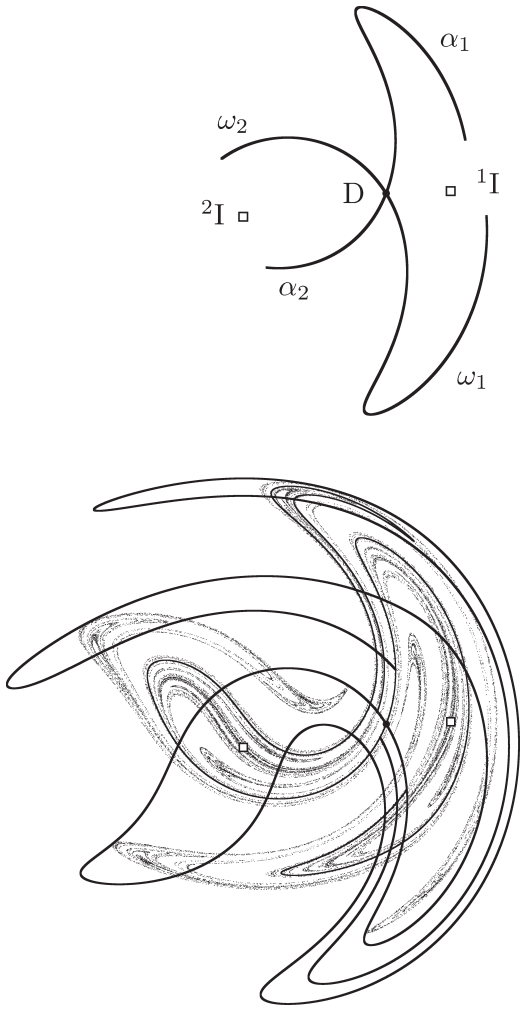

Figure 3. Invariant branches of the saddle fixed point D on UCA

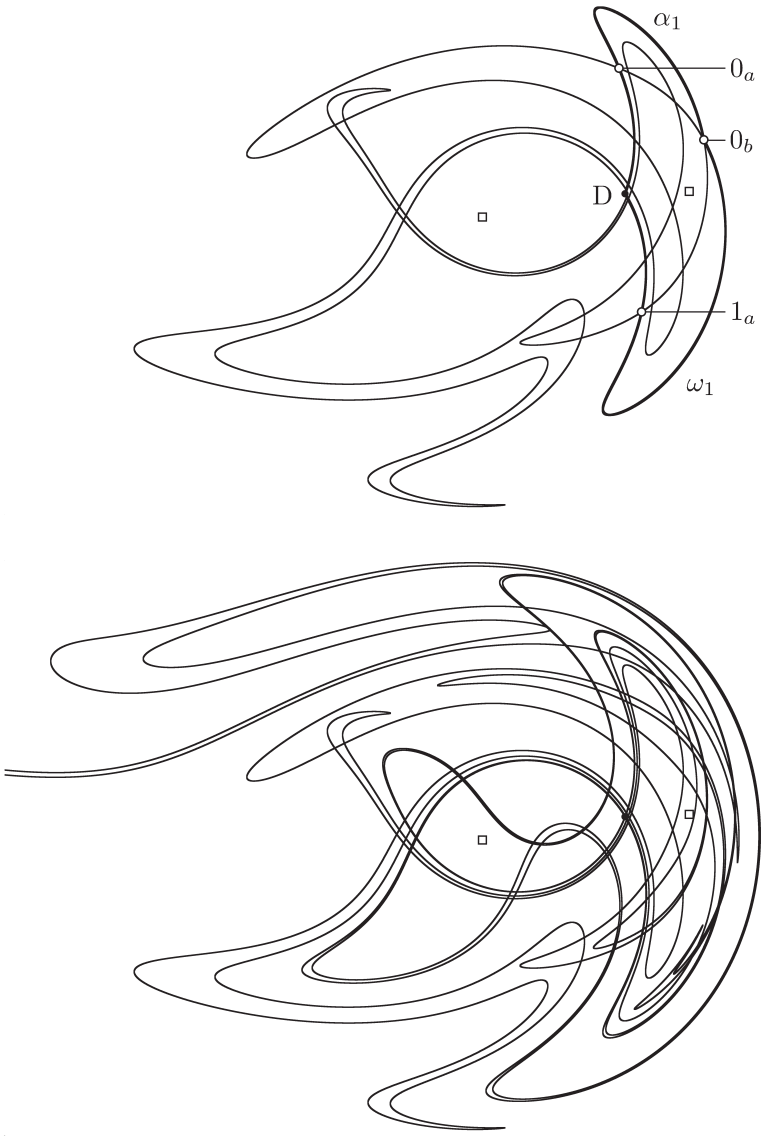

Figure 4(a). α_1, ω_1 homoclinic structure (Type A)

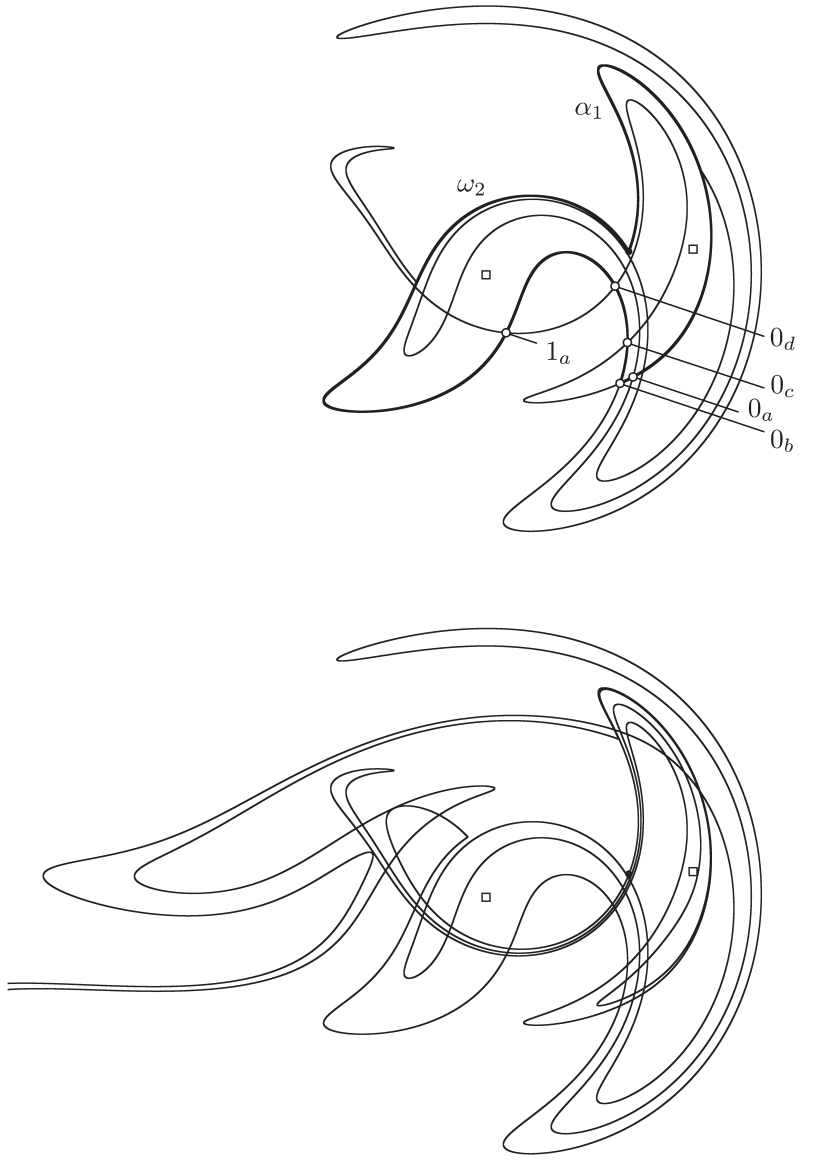

Figure 4(b). α_1, ω_2 homoclinic structure (Type B)

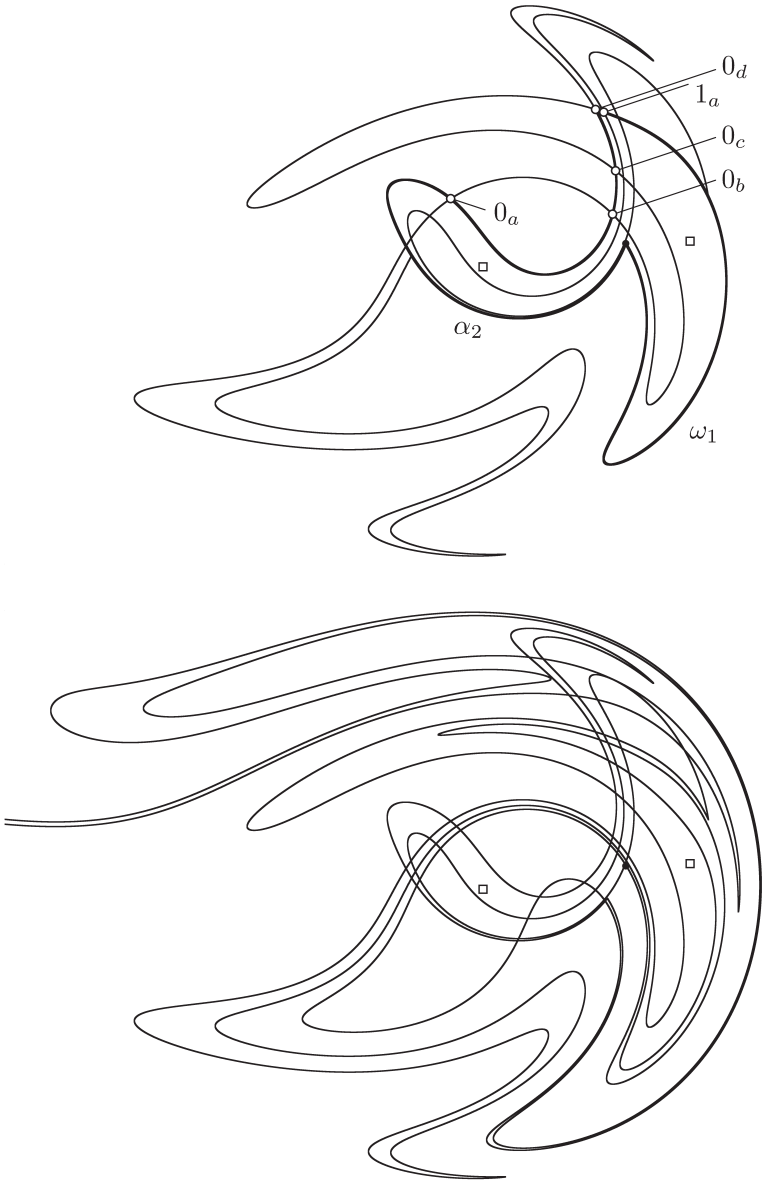

Figure 4(c). α_2, ω_1 homoclinic structure (Type C)

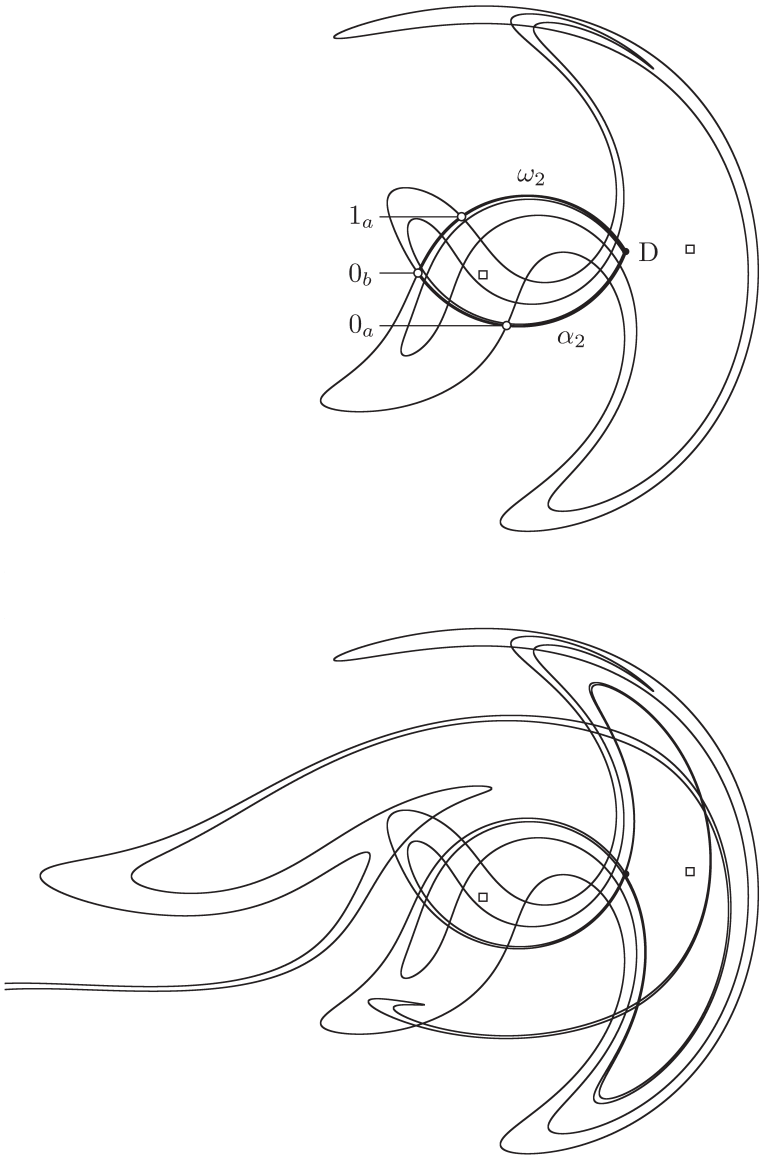

Figure 4(d). α_2, ω_2 homoclinic structure (Type D)

Figure 5. Prototypical homoclinic structure of UCA system

Figure 6. Evidence of the existence of special-type d.a. points on UCA

Background of this document release

As mentioned at the beginning of this article, last year the author published "Theory of Chaotically Transitional Phenomena (in Japanese)". At that time, international mail was dormant in the midst of the COVID-19 pandemic, and the author did not send the book to my friends overseas, taking into consideration the problem of a Japanese-language book.

However, it was sent only to Ralph-san in the summer, when the postal situation began to ease up. At the time, he was immersed in an electronic publication project of an old book we had edited together [*34]. His goal was to publish Robert May's contribution in an electronic version [*35]. He also encouraged the author to contribute a new chapter. This English abridgment was undertaken under these circumstances.

It was early spring of 2022, when Professor Ken Umeno of Kyoto University, who presides over the Applied Chaos Field of JSIAM, inquired about the possibility of establishing the Ueda Yoshisuke Prize to honor young researchers in the field of chaos at the Japan Society for Applied Mathematics. For this purpose, he asked me to approve the use of my name.

At that time, I immediately felt "Is it appropriate for my name to be endorsed by such an award?" It would be a great honor, but it would also call into question not only my academic achievements but also my character as a person. I have no certainty. However, I realized that the evaluation and judgment would be made by others (there is no room for my involvement), so I decided to

---

[*34] Editos, Ralph Abraham and Yoshisuke Ueda, "*The Chaos Avant-Garde: Memories of the Early Days of Chaos Theory",* Contributors: Steve Smale, Yoshisuke Ueda, Ralph Abraham, Edward Lorenz, Christian Mira, Floris Takens, T. Y. Li and James A. Yorke, Otto E. Rössler, World Scientific Publishing Co. Pte. Ltd., Singapore (2000).

[*35] Ralph-san has a very high regard for Robert May's paper in the history of chaos theory. We asked him to contribute to this article in 1999, just before May-san assumed the presidency of the Royal Society 2000-2005. At that time, May-san declined due to pressures on his time.

We received a contribution from May-san after the co-edited book was published (May-san passed away in 2020). This Japanese translation is included in the bibliography below:

ラルフ・エイブラハム　ヨシスケ・ウエダ編著、稲垣 耕作、赤松 則男訳、
『カオスはこうして発見された』、共立出版株式会社 (2002).

leave it to the people involved. Afterwards, Professor Umeno reported that the Ueda Yoshisuke Award had been established and that the selection of the first recipient had been completed. I think it was at that time that he mentioned the need for publicity to let many people know that the Ueda Yoshisuke Prize had been established.

In the early summer of 2023, Professor Umeno asked me about the possibility of contributing to the website of the Japan Society for Applied Mathematics in the field of Applied Chaos, which was under planning. At that time, I was in the final stages (proofreading) of the digitization project with Ralph-san, so I gave a vague reply. However, shortly thereafter, in June 2023, unfortunately, the digitization project that Ralph had intended to pursue had to be postponed due to issues related to the copyright of the original book.

As described above, an abridged English translation of my book will be contributed to the website of the Applied Chaos Division of the Japanese Society for Applied Mathematics.

On a different note, allow me to describe some of the memorable events that have taken place during this period.

In the summer of 2022, the author received an unexpected piece of good fortune "the 2023 IEEE Technical Field Award" [*36]. When I was asked if I would attend the May 2023 award ceremony (in Monterey, California, USA), I replied that unfortunately I would not be able to attend. However, "the

[*36] 2023 IEEE GUSTAV ROBERT KIRCHHOFF AWARD
YOSHISUKE UEDA
For the discovery of chaotic phenomena in electronic circuits and for contributions to the development of nonlinear dynamics.
Sponsored by the IEEE Circuits and Systems Society

Yoshisuke Ueda has made fundamental and sustained contributions to the field of chaotic phenomena. He was the first to show experimental evidence that chaotic phenomena were possible in electronic circuits calling his discovery a "broken-egg" attractor. In the decades that followed, research activity on the theory and application of chaos flourished and brought significant breakthroughs to areas of communication and cryptography. Recent research on neural networks are based on nonlinear coupled circuits, where the existence of chaos is one of the most important features of their functional capabilities. Ueda developed effective methods to distinguish chaotic phenomena from other complex experimental observations, through phase portraits, bifurcation diagrams, and spectrum and basin analysis.

Ueda is a professor emeritus at Kyoto University.

author's award ceremony" was held in conjunction with the opening ceremony of the 28th Asia and South Pacific Design Automation Conference (ASP-DAC) in Tokyo in January 2023.

Acknowledgments

First of all, the the author would like to express his deepest respect and gratitude to all those who have contributed to the establishment and development of nonlinear science.

Over the years, the author has wandered in the hands of Poincaré, Birkhoff, Smith, Levinson, Lyapunov, Andronov, Pontryagin, Duffing, Van der Pol, and others. The joy of having been able to guess over the years and subtly perceive how they came up with such an idea has made the author realize the depth of their work beyond expression.

The author would like to recognize their achievements as the source and guiding principle of this research, and would like to express his sincere respect and gratitude to them. Thank you very much. With a sense of respect, the author has omitted the titles attached to the proper nouns.

The fact that the author received the 2023 IEEE Gustav Robert Kirchhoff Award and that the award ceremony was held in Tokyo was noted above. The realization of the award ceremony in this way was made possible not only by the goodwill of the people involved, but also through many tedious meetings and procedures. The main roles were played by Mr. April Compertore of the IEEE Award Group, Prof. Atsushi Takahashi and Prof. Emeritus Akinori Nishihara of Tokyo Institute of Technology, and Professor Takashi Hikihara of Kyoto University.

The electronic publication of this abridged translation came about as a result of a plan by Professor Emeritus Ralph Abraham (University of California, Santa Cruz). The outline of the process was mentioned above, and the author would like to thank his longtime and esteemed friend Ralph-san for his encouragement, many helpful suggestions, and even advice on the selection of the title of the article.

The author is grateful to Prof. Takaya Miyano for his many helpful suggestions in the writing of the manuscript. He and the author have enjoyed thier monthly "research discussion meetings" for the past several years. The "dis-

cussion meeting" is an opportunity to talk frankly with each other about any questions that concern them, without being ashamed of thier ignorance. Even if you cannot get the right answer, it is very effective to talk about your stuck problems, unclear and uncertain understandings, ···, and the results of the conversations are embedded in many parts of the manuscript.

Furthermore, as mentioned above, Professor Ken Umeno of Kyoto University has made a great effort to publish this English translation on the website of the Japan Society for Applied Mathematics and the Division of Applied Chaos.

The author would like to express his sincere and heartfelt thanks to all those who have been mentioned by proper name.

The IEICEJ Nolta Society and the Foundations and Boundaries Society hosted a lecture by the author in commemoration of the 2023 IEEE Gustav Robert Kirchhoff Award (October 13). In addition, the IEICE ICT Pioneers Webinar Series (43rd) was held on October 27 using the recorded video of the lecture. I would like to express my gratitude for the efforts of many people involved in this series of events. In particular, I would like to express my deepest gratitude to President Mikio Hasegawa of the Nolta Society, who took care of everything from planning to implementation and even edited the troublesome video (this paragraph was slipped in when I was proofreading a JSIAM contributed paper).

As those of you who know him well may have guessed, the author has little memory of taking care of his parents, let alone housework, or playing with his grandchildren, and without the understanding and cooperation of his wife Miyoko, this work would never have seen the light of day. The author would like to express his deepest gratitude to her.

Finally, the author would like to thank the DeepL translation tool for its assistance in translating this abstract into English. The author would like to "express his gratitude" here. However, the author's usage will not be thrown into the tool. The author's poor English skills have been used to rewrite the text in some places. In other words, the author is responsible for any problems with the English wording.